ORIGINAL ARTICLE

Development of a numerical model to simulate the behavior of plate shear connectors applied to slender cross-section concrete-filled steel tube

Desenvolvimento de um modelo numérico para simular o comportamento de conectores em chapa aplicados a pilares mistos preenchidos com concreto de seção esbelta

Ariany Cardoso Pereira[a]
Larice Gomes Justino Miranda[a]
Lucas Ribeiro dos Santos[a]
Rodrigo Barreto Caldas[a]

[a]Universidade Federal de Minas Gerais – UFMG, Departamento de Engenharia de Estruturas, Belo Horizonte, MG, Brasil

Abstract: The cross-section of concrete-filled steel tube (CFST) columns is classified according to the local slenderness of the steel tube as slender, non-compact, or compact. There are analytical models to determine the axial force of locally slender CFST columns, however studies on load transfer from beams connected to these columns are scarce. This paper presents the process of the development and validation of a numerical model to simulate the behavior of Crestbond connectors applied to CFST columns with slender steel tubes, based on the results of experiments carried out. The numerical model presented can be used for the analysis and design of the load transfer in slender columns using connectors known as composite dowels.

Keywords: Crestbond connector, load transfer device, CFST, composite dowels.

Resumo: Os pilares mistos preenchidos com concreto (PMPC) podem ter a seção transversal classificada em função da esbeltez local do perfil tubular como sendo: esbelta, semicompacta ou compacta. Embora já existam modelos de cálculo para determinação da força axial resistente dos PMPC com seção tubular esbelta, são escassos os estudos sobre a transferência de forças vindas das vigas conectadas a esses pilares. Este artigo tem como objetivo apresentar o processo de desenvolvimento e validação de um modelo numérico para simular o comportamento dos conectores Crestbond aplicados a (PMPC) de seção tubular esbelta, com base em resultados de experimentos realizados. O modelo numérico apresentado pode ser utilizado para o estudo e projeto da transferência de força em pilares de seção esbelta utilizando conectores em chapa conhecidos como *composite dowels*.

Palavras-chave: conector Crestbond, transferência de carga, PMPC, composite dowels.

1 INTRODUCTION

The competitiveness and applicability of concrete-filled steel tubes (CFST) columns are associated with the interaction between the steel tube and the concrete core and the difficulty to connect them to the beams. In this way, when the shear stress exceeds the natural bond strength between the steel tube and the concrete core, it is necessary

to apply mechanical devices such as shear connectors. Among the devices standardized by ABNT NBR 8800:2008 [1], there are stud bolts and by ABNT NBR 16239:2013 [2], there are bolted shear connectors. Several studies on the load transfer through these connectors have already been carried out, including De Nardin and El Debs [3] and Santos et al. [4]

The behavior of the concrete-filled steel tubes (CFST) columns is also influenced by the local slenderness of the composite cross section (λ), since it is a function of the ratio between the diameter (or side, for rectangular sections) and the thickness of the tube [5]–[7]. The American standard AISC 360-16 [8] classifies CFSTs according to the local slenderness of the cross section. According to this standard, the cross section can be classified as being slender, non-compact or compact, providing the design recommendations for determining their axial strength. However, the load transfer from the beams connected to these columns still has few studies and solutions.

De Nardin and El Debs [3] verified the contribution of stud bolts, in the shear strength in the steel-concrete interface in CFST columns submitted to push-out tests. Starossek et al. [5] and Cardoso [9] experimentally evaluated the rupture mode of CFST columns subjected to an axial load while using stud bolts as shear connectors, proving the efficiency of bolted shear connectors for such application. Cardoso [9] experimental results later served as basis for studies by Santos [10] and Prates [11]. Santos [10] proposed a new analytical model to describe the behavior of bolted shear connectors when used as shear connectors in CFST. Prates [11] studied the behavior of bolted shear connectors, when used as shear connectors in columns composed of cold formed steel tubes filled with concrete, a simple and innovative solution for this type of connection, eliminating welding. The load transfer in the CFST by bolted shear connectors was also the study object of Ribeiro and Sarmanho [12] and Xavier et al. [13] Younes et al. [14] and Tao et al. [15], who evaluated the load transferred using bolted connectors in CFST columns subjected to axial and cyclical loads, respectively. Although the way in which force is applied is different, Younes et al. [14] as for Tao et al. [15] also corroborated the efficiency of this type of tool as shear connector in CFST columns.

The Crestbond connector initially studied for application in beams [16], began to be tested as a load transfer device in CSFT columns. The Crestbond dowels allow compatibility with the reinforcement rebars of the CSFT columns, and its steel plate can be designed to integrate with a beam-column connection (Figure 1).
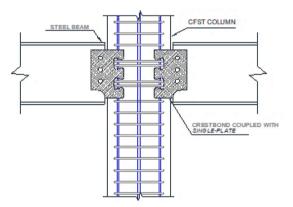

Figure 1. Crestbond connector with single plate extension for connection with beams [Caldas et al. [17]

Different studies carried out by researchers at the School of Engineering at Universidade Federal de Minas Gerais (UFMG) prove the efficiency of the Crestbond connector to be used as a shear load transfer device in compact section CFST columns [17]–[19]

After the efficiency of the Crestbond connector in application in CFST columns was proven, both the behavior of the Crestbond connector and the composite cross section started to be analyzed in specific ways. In this context, the present study aimed to develop and validate a numerical model to analyze the shear load transfer in locally slender composite CFST columns with the Crestbond connector.

2 EXPERIMENTAL PROGRAM

Two shear tests were carried out in order to experimentally evaluate the behavior of the Crestbond shear connector when used as load transfer device in slender section of the CFST columns. The execution of the tests was defined by

adapting the standard shear test procedures (push-test) prescribed in Annex B of the European Standard EN 1994-1-1:2004 [20]

As in Cardoso [18] experiments, the displacement of the CFST was restricted, while the steel tube was kept free to slide in relation to the concrete core. In addition, a release agent was applied to the internal surface of the steel tubes to minimize friction at the material interface, causing the force in the section to be transmitted, mainly, through the Crestbond CR56b-R12 shear connectors with the geometric pattern proposed by Verissimo [16] The relative displacement between the steel tube and the concrete core was measured using displacement transducers (DTs) fixed vertically in strategic positions to capture linear displacements between the tube and the concrete. From the force versus vertical relative displacement curves obtained experimentally, it was possible to develop the numerical models of the present study.

2.1 Compact cross section CFST

In the study by Cardoso [18], the CFST models with Crestbond shear connectors had compact tubular cross sections (local slenderness limited to $34 \le \lambda \le 40$) and had the force applied to the steel tube through a set of end-plates (Figure 2). The prototypes were 100 cm high with a gap of 5 cm between the top of the concrete core and the plate for applying force to the test device. The configurations of the shear test can be seen in Figure 2.
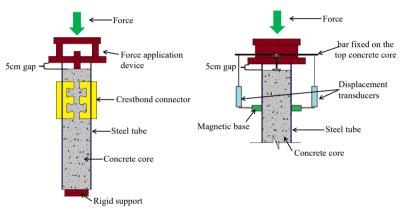

Figure 2. Schematic illustration of test-setup [18]

2.2 Slender cross section CFST

The authors experimentally evaluated the behavior of the Crestbond connector applied to slender section CFST (local slenderness equal to 153) and, due to the great local slenderness of the steel tubes, a new shear test methodology was developed [21] In this test program, the force was introduced directly into a Crestbond connector.

The CFSTs were 75 cm high and were locked by end-plates rigid enough to prevent rotation of the model that had a Crestbond with two steel dowels (CR2D). The configurations of the shear test can be seen in Figure 3.
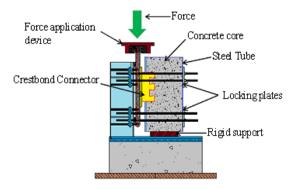

Figure 3. Schematic illustration of test-setup [21]

The configuration of the tested models can be seen in Figure 4 and their geometrical properties are shown in Table 1.
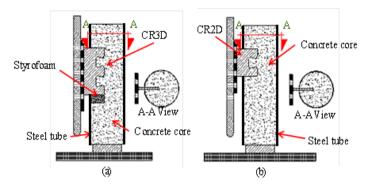

Figure 4. Schematic illustration: (a) C Model; (b) E Model.

The present study has the purpose to develop a finite element model able to simulate the behavior of Crestbond connectors applied in thin-walled CFST columns. Among the studies previously presented Cardoso (2018) was the principal reference by this work, because it analyzed CFST columns with compact cross-section using the same connectors.

The numerical results of Cardoso [18] were good from a numerical study calibrated based on an experimental analysis realized with more than 20 models. In this sense, the present study aims to be a continuation of the work started by Cardoso [18], but now to evaluate the slender thin-walled CFST columns tested in the same laboratory and developed by the same research group.

So, the experimental models studied by Cardoso [18] are present in Table 1 with the experimental models of the present work, because these models together formed the basis of the numerical model developed.

Table 1. Experimental model configuration

Ref.	Model	Tube section	Dimensions (mm)	Steel tube	λ*	Connection description	Steel connection
Cardoso [18]	S1-04CR	Circular	219.1 x 6.4	VMB 350	34	$4\times(3D_a+2D_c+F)$	USI CIVIL 350
	S1-02CR	Circular	219.1 x 6.4	VMB 350	34	$2\times(3D_a+2D_c+F)$	USI CIVIL 350
	S1-02CR-ConA	Circular	219.1 x 6.4	VMB 350	34	$2\times(3D_a+2D_c+F)$	USI CIVIL 350
	S1-02CR-E	Circular	219.1 x 6.4	VMB 350	34	$2\times(3D_a+2D_c+F)$	USI CIVIL 350
	S1-02CR-2D	Circular	219.1 x 6.4	VMB 350	34	$2\times(4D_a+3D_c+F)$	USI CIVIL 350
	S2-02CR	Circular	355.6 x 9.5	VMB 250	37	$2\times(3D_a+2D_c+F)$	USI CIVIL 350
	S2-02CR-E**	Circular	355.6 x 9.5	VMB 250	37	$2\times(3D_a+2D_c+F)$	USI CIVIL 350
	S3-02CR	Rectangular	320 x 250 x 8.2	VMB 250	39	$2\times(3D_a+2D_c+F)$	USI CIVIL 350
	S3-02CR-E	Rectangular	320 x 250 x 8.2	VMB 250	39	$2\times(3D_a+2D_c+F)$	USI CIVIL 350
Current work	C**	Circular	230 x 1.50	SAE J403 1010	153	$1\times(3D_a+2D_c+SF)$	ASTM A1018
	E**	Circular	230 x 1.50	SAE J403 1010	153	$1\times(2D_a+1D_c+F)$	ASTM A1018

*λ represents the thinness index of the cross section of the composite column | ** This series features only one model | S1 - Section 219.1 x 6.4 | S2 - Section 355.6 x 9.5 | S3 - Section 320 x 250 x 8.2 | CR - Crestbond Connector | Da - number of steel dowels | Dc - number of concrete dowels | F - Concrete frontal strength | SF - Without concrete frontal strength | ConA - Self-compacting concrete | E - Stirrup | | The S1-02CR-E models; S2-02CR-E and S3-02CR-E had internal reinforcement

From the data obtained during the tests, the curves Force (kN) x Relative Displacement (mm) shown in Figure 5 and Table 2 were obtained.
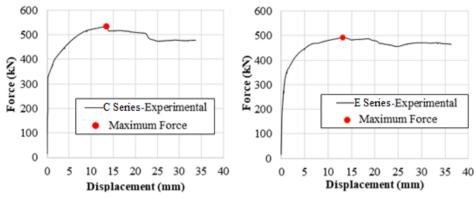
Figure 5. Force (kN) x Relative Displacement (mm) of the experimental models.

Table 2. Force and displacement numbers acquired from tests

Model	Maximum Force (kN)	Displacement at Maximum Force (mm)
C Series	535.24	13.39
E Series	492.99	13.16

3 FINITE ELEMENT MODEL

3.1 Generalities

The numerical analysis was developed using the finite element program ABAQUS - version 6.14. The numerical model was elaborated with the same parameters adopted in the study by Cardoso [18] The final shape of the numerical models can be seen in Figure 6.
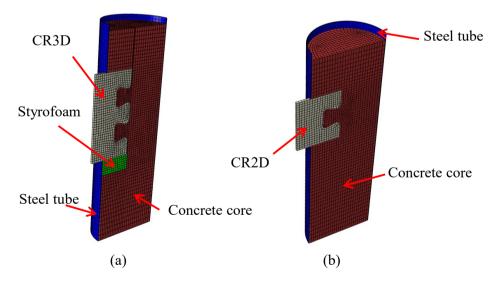

(a)   (b)

Figure 6. Numerical model overview: (a) SerieC Model and (b) SerieE Model.

3.2 Finite Element Mesh

The mesh elements adopted for the modeling of the steel tube, concrete and connector were of the C3D8 type (Continuum, hexahedral and linear), a type of solid element that has eight nodes (only at the vertices) with three degrees of freedom per node (translations in the three main directions X, Y and Z). This element is shown in Figure 7.
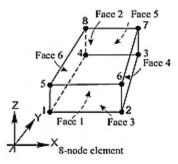
Figure 7. C3D8 Mesh Element [19]

The sizes of the mesh elements were defined through a study of mesh sensitivity and refinement and its discretization are illustrated in Figure 8. In Crestbond and in the region limited by around the shear connectors, mesh elements with a length of 8 mm (II) were used, which was increased as the elements moved away from the region of concentration of efforts. For the concrete and tube located in the upper region of the connector, mesh elements with a length varying between 10 mm and 15 mm (I) were applied. For the parts located in the region below the connector, the mesh was divided into elements with a length varying between 10 mm and 20 mm (III). Finally, mesh elements with a width of 10 mm were chosen for the direction corresponding to the model's transversal axis (IV).
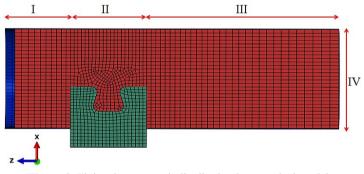

Figure 8. Finite element mesh distribution in numerical models.

The mesh distribution methods adopted were structured mesh and sweep mesh. Due to the complexity of the model, divisions were made to favor the allocation of the finite element mesh and are shown in Figure 9.
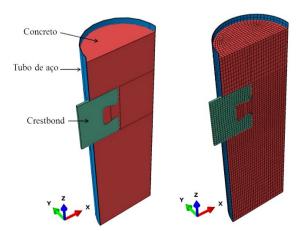

Figure 9. Divisions and finite element mesh adopted in numerical models

A. C. Pereira, L. G. J. Miranda, L. R. Santos, and R. B. Caldas

Based on the studies carried out by Santos [21] and Cardoso [18], the contact between concrete, steel profile and shear connector was simulated considering a static friction coefficient of 0.5 for the contact between the connector and the concrete, 1.0 between the connector and tube, and 0.17 between the tube and the concrete core. It was considered that in the test the friction between the steel tube and the concrete was minimized with paint and the release agent inside the tube.

The contact between concrete, steel tube and shear connectors, was simulated through face-to-face interactions and it was necessary to define separately in each contacts pairs which was the stiffer element. The rigid type of contact was defined in all the interactions which is the one that admits the minimum penetration between the surfaces of the elements. The contact pairs on the surfaces were defined as: Concrete-to-Tube (Figure 10a); Concrete-to-Connector (Figure 10b); Tube-Connector (Figure 10c).
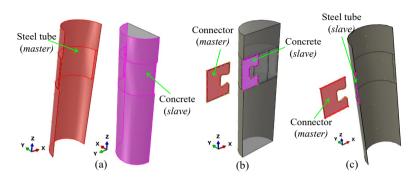

Figure 10. Perspective view of the contact pairs of the numerical models: (a) Concrete-to-Tube; (b) Crestbond-to-Concrete; (c) Connector-to-Tube.

3.2.1 Boundary Conditions

To reproduce the test conditions, the following boundary conditions were adopted: (I) restriction of the concrete core to vertical displacement to simulate the rigid support of the test; (II) rotation and horizontal displacement restrictions to represent the symmetry of the real model and (III) springs with stiffness (k) calculated in order to simulate the stiffness of the locking plates of the experimental model. The boundary conditions are shown in Figure 11.
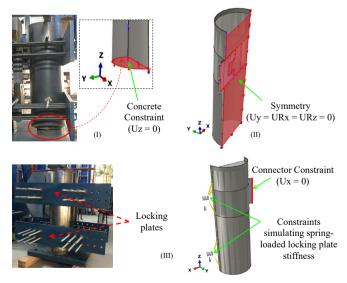

Figure 11. Boundaries Conditions of the Numerical Models.

3.2.2 Displacement Application and Data Acquisition

To simulate the monotonic loading with displacement control of the experimental test and to avoid possible convergence problems, it was decided to introduce displacement increments and obtain the corresponding reaction forces to get the force versus displacement curve of the model.

For this purpose, a reference node was created, called as Reference Point (RP) connected to the Crestbond connector plate, as shown in Figure 12. In this way, as each increment was applied, the connector moved and, because of the rigid connection with the other materials of the model, transferred the displacement in the section. In addition, it is important to note that numerical data acquisition was also carried out through the RP.
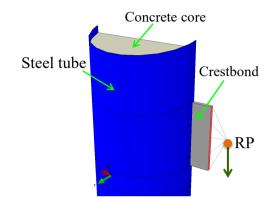

Figure 12. Displacement insertion point in the numerical model

For the nonlinear analysis of the models, the Dynamic Implicit analysis method was used with the quasi-static option. This method was used by Santos [10] and Cardoso [18] and it shows good convergence and satisfactory results, proving to be efficient for the analysis of shear connectors applied in CFST columns.

3.2.3 Concrete Constitutive Model

The Concrete Damaged Plasticity model (CDP) was used for the simulate the concrete core constitutive model and it is available in the ABAQUS library. This model is suitable for modeling fragile materials and has been widely applied for numerical modeling involving confined concrete.

The input parameters required for this model are the dilatation angle (ψ); the ratio between the compressive yield stress in the biaxial and uniaxial state (σ_{b0}/σ_c); the ratio between the second invariant stress of the tension meridian and the second invariant stress of the compression meridian (K_c); viscosity parameter (μ_{vis}); and the eccentricity (ϵ). Based on the studies by Aguiar [22] and Cardoso [18], in this work adopted: $\psi = 36°$, $\sigma_{b0}/\sigma_c = 1.16$, $K_c = 2/3$, $\mu_{vis} = 0.00005$ and $\epsilon = 0.1$.

To represent the behavior of the confined concrete subjected to compression, it was adopted the stress versus strain relationship, proposed by Pavlović et al. [19] illustrated in Figure 13.
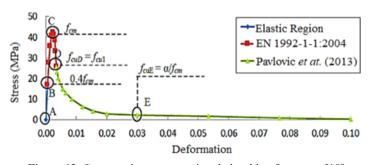

Figure 13. Compressive stress-strain relationship of concrete [18]

Rev. IBRACON Estrut. Mater., vol. 16, no. 1, e16108, 2023

8/16

Pavlović et al. [19] proposed a continuous sinusoidal curve that starts at the point D, presented by the European standard EN 1992-1-1:2004, and continues until the strain $\varepsilon_{cu} = 0.01$, defined by the following equation:

$$\sigma_c = \begin{cases} f_{cm}\left[\dfrac{1}{\beta} - \dfrac{sen\left(\frac{\mu\alpha_{tD}\alpha_{tE}\pi}{2}\right)}{\beta sen\left(\frac{\alpha_{tE}\pi}{2}\right)} + \dfrac{\mu}{\alpha}\right], & \varepsilon_{cuD} < \varepsilon_c \le \varepsilon_{cuE} \\ \dfrac{f_{cuE}(\varepsilon_{cuF}-\varepsilon_c)+f_{cuF}(\varepsilon_c-\varepsilon_{cuE})}{(\varepsilon_{cuF}-\varepsilon_{cuE})}, & \varepsilon_c > \varepsilon_{cuE} \end{cases} \tag{3.1}$$

where, $\mu = (\varepsilon_c - \varepsilon_{cuD})/(\varepsilon_{cuE} - \varepsilon_{cuD})$.

The stresses at the D and E points are defined as $f_{cuD} = f_{cu1} = \sigma_c(\varepsilon_{cu1})$; $f_{cuE} = \alpha/f_{cm}$. Strains at the D and E points are defined as $\varepsilon_{cuD} = \varepsilon_{cu1}$; $\varepsilon_{cuE} = 0.03$, respectively. The remaining parameters are defined as: $\alpha = 20$, $\alpha_{tD} = 0.5$, $\alpha_{tE} = 0.10$ e $\beta = f_{cm}/f_{cu1}$.

To reproduce the behavior of concrete under tension, the same curve used in Cardoso numerical study was adopted in this work [18] This author used the stress curve (σ_t) versus crack opening (W$_c$) proposed by Tahmasebinia et al. [23], as in Figure 14.

The damage variables d_c (damage to uniaxial compression) and d_t (damage to uniaxial tension), were calculated, where $d_c = 1 - \dfrac{\sigma_c}{f_{cm}}$ e $d_t = 1 - \dfrac{\sigma_t}{f_{ctm}}$ [23], and inserted in the ABAQUS program according to the plastic deformations equivalent to tension and compression, respectively.
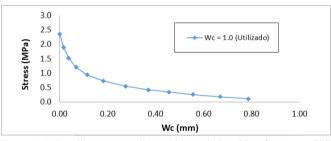

Figure 14. Tensile stress-crack openings relationship of concrete [23]

3.2.4 Tube and Connector Steel Constitutive Model

To simulate the steel behavior of the connectors and the tubes, an elastoplastic model with hardening was adopted based on the multilinear theoretical diagram in Figure 15. This model was used by Cardoso [18] The part of the graph that represents the smooth unloading (G-H in Figure 15) was adopted as a numerical solution to complete the analysis in a regime of large deformations.

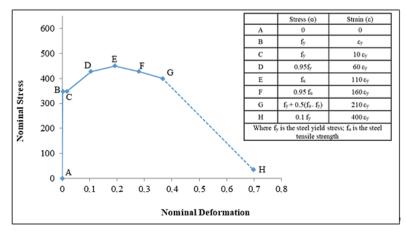|	Stress (σ)	Strain (ε)
A	0	0
B	f_y	ε_y
C	f_y	$10\,\varepsilon_y$
D	$0.95f_y$	$60\,\varepsilon_y$
E	f_a	$110\,\varepsilon_y$
F	$0.95\,f_a$	$160\,\varepsilon_y$
G	$f_y + 0.5(f_a - f_y)$	$210\,\varepsilon_y$
H	$0.1\,f_y$	$400\,\varepsilon_y$
Where f_y is the steel yield stress; f_a is the steel tensile strength		

Figure 15. Steel stress-strain relationship for steel elements

3.3 Numerical Model Validation and Analysis of the Results

3.3.1 Generalities

The same characteristics were adopted as in Item 2.2 with the exception for the fictitious springs that were added to the numerical model to represent the locking plate of the test device, as illustrated in Figure 16a.
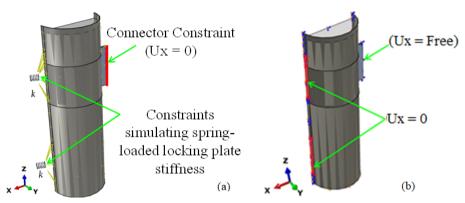

Figure 16. Change in boundary conditions: (a) Original model (with spring), (b) Modified model (without spring).

The numerical results were validated by comparing them to the force versus relative displacement curve obtained experimentally, evaluating the initial stiffness, the maximum force value obtained in the analyzes and the deformed configuration of the models.

Figure 17 shows the comparison between the numerical and experimental curves of the analyzed models. By comparing the curves, it is possible to observe that the numerical results were close to the experimental ones.
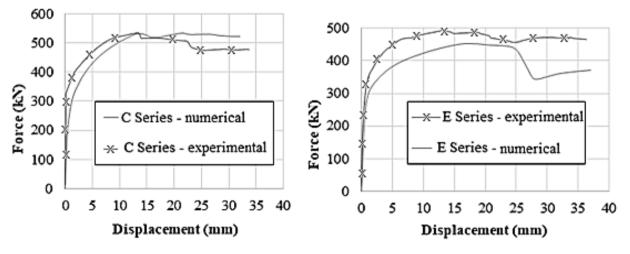

Figure 17. Numerical and experimental curves: C Series Model and E Series Model.

The slope of the two curves of model E practically overlapped, where the numerical model ensured the representation of a connection with an initial stiffness close to that obtained experimentally. In addition, it is observed that in C Series Model numerical curve practically coincided with the maximum force and E Series Model remained below the experimental curve, demonstrating a more conservative numerical model than the experimental one, as in Tables 3 and 4.

Rev. IBRACON Estrut. Mater., vol. 16, no. 1, e16108, 2023

10/16

Table 3. Comparison between numerical and experimental results: C Series Model

	Experimental	Numerical
Maximum force (kN)	535.24	533.12
Displacement at maximum force (mm)	13.39	21.53
Maximum displacement (mm)	33.71	32.04
Difference from the experimental[1]		0.40%

[1] Defined at numerical model

Table 4. Comparison between numerical and experimental results: E Series Model

	Experimental	Numerical
Maximum force (kN)	493.00	452.46
Displacement at maximum force (mm)	13.16	17.56
Maximum displacement (mm)	36.32	37.00[1]
Difference from the experimental [2]		8%

[1]Defined at numerical model. [2] Difference between the maximum force values obtained in the numerical model and in the test

For both analyzes, a good correlation was observed between the deformations of the connectors in the numerical and experimental models, as shown in Figures 18 and 19.
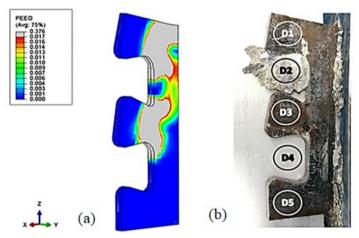

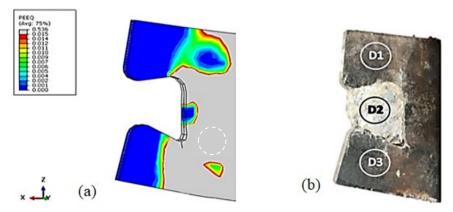**Figure 18.** Deformed shaped for C Series Model: (a) Numerical Model; (b) Model after testing

Figure 19. Deformed shaped for E Series Model (a) Numerical Model; (b) Model after testing

Figure 20 shows images of the numerical and experimental C series model after testing. The numerical model was able to reproduce where the concrete damage was more pronounced like the observed in the experimental analysis. For that, the results for the variable DamageT, which represents the degradation of the concrete tensile stiffness, are evaluated in the numerical model. The red region indicates a complete no stiffness, which culminated in the separation of the concrete core by tensile stresses.
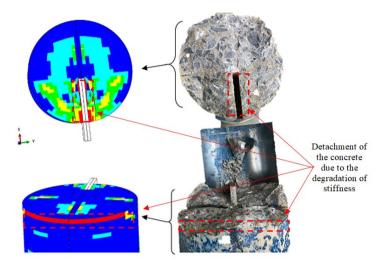

Figure 20. Deformed shaped for C series model: representation of the concrete cracking pattern

3.4 Model Geometry Transition

To simplify the numerical model so that the simulation time and the computational cost of the analyzes were lower, some sensitivity tests were necessary to validate the transition of the model geometry, including the removal of the springs and the evaluation of the model behavior with two symmetries.

3.4.1 Sensitivity Test of the Locking Plate Stiffness

To enable the analysis of 1/4 of the numerical model, it was necessary to remove the springs that simulated the locking plates in the test. In addition to simplifying the model, considering zero stiffness for springs allows simulating situations more similar that occur in reality, in which there is less restriction for the connector. For that, the boundary conditions were modified, releasing the horizontal translation of the plate of the connector and restricting the regions corresponding to the location of the locking plates, as shown in Figure 16.

From the results obtained, it was possible to observe that the removal of the spring led to a more conservative model, favoring safety, shown in Figure 21 and Tables 5 and 6.
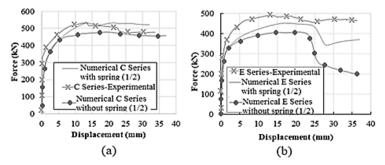

Figure 21. Experimental and numerical curves with and without springs: (a) C Series model and (b) E Series model

Rev. IBRACON Estrut. Mater., vol. 16, no. 1, e16108, 2023

12/16

Table 5. Comparison between experimental and numerical results (with and without springs): C Series Model

	Experimental	Numerical	
		Springs	No springs
Maximum force (kN)	535.24	533.12	478.8
Displacement at maximum force (mm)	13.39	21.53	19.23
Maximum displacement (mm)	33.71	32.07	37.00[1]
Difference from the experimental [2]		0.40%	10.54%

[1] Defined at numerical model. [2] Difference between the maximum force values obtained in the numerical model and in the test

Table 6. Comparison between experimental and numerical results (with and without spring): E Series Model

	Experimental	Numerical	
		Springs	No Springs
Maximum force (kN)	493.00	452.46	408.06
Displacement at maximum force (mm)	13.16	17.56	20.86
Maximum displacement (mm)	36.32	37.00[1]	37.00[1]
Difference from the experimental [2]		8%	17%

[1] Defined at numerical model. [2] Difference between the maximum force values obtained in the numerical model and in the test

3.4.2 Sensitivity Test of Transition to Double Symmetry

As concluded the evaluations that proved the possibility of removing the springs that simulated the locking plates and after observing that the curves remained more conservative (below the experimental curve), a sensitivity test was performed for the double symmetry, allowing the modeling only 1/4 of the model, illustrated in Figure 22. The model reduction to 1/4 provided more conservative results (Figure 23 and Tables 7 and 8). Furthermore, there was a reduction in processing time per model with 1/4 configuration without springs of about 10 hours, in relation to the time required for the simulation of 1/2 models with spring. Thus, it was adopted the numerical 1/4 model without springs to be used in parametric studies and analytical models of shear load transfer in slender composite sections columns through Crestbond connectors.
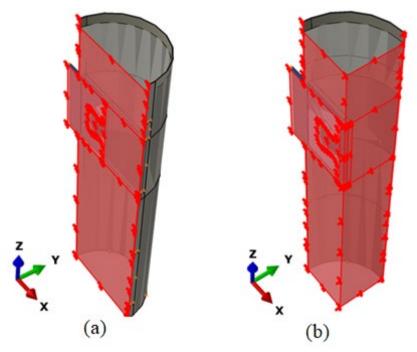

Figure 22. Geometry transition: (a) Original model (a plane of symmetry), (b) Modified model (double plane of symmetry)

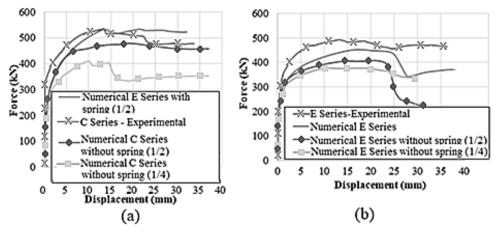Rev. IBRACON Estrut. Mater., vol. 16, no. 1, e16108, 2023

13/16

Figure 23. Experimental and numeric curves with springs, without springs (1/2) and without springs (1/4): C Series Model and E Series Model.

Table 7. Comparison between experimental and numerical results (without spring (1/2) and without spring (1/4)): C Series Model

	Experimental	Numerical	
		No springs (1/2)	No springs (1/4)
Maximum force (kN)	535.24	478.80	410.15
Displacement at maximum force (mm)	13.39	20.86	10.98
Maximum displacement (mm)	33.71	37.00[1]	37.00[1]
Difference from the experimental [2]		11%	23%

[1] Defined at numerical model. [2] Difference between the maximum force values obtained in the numerical model and in the test

Table 8. Comparison between experimental and numerical results (without spring (1/2) and without spring (1/4)): E Series Model

	Experimental	Numerical	
		No springs (1/2)	No springs (1/4)
Maximum force (kN)	493.00	408.06	377.52
Displacement at maximum force (mm)	13.16	20.86	10.98
Maximum displacement (mm)	36.32	37.00[1]	30.08
Difference from the experimental [2]		17%	23%

[1] Defined at numerical model. [2] Difference between the maximum force values obtained in the numerical model and in the test

4 CONCLUSIONS

This work presents the development of a numerical model to simulate the behavior of a Crestbond shear connector applied in CFST columns with slender composite section. Although analytical models for determining the axial strength of CFST already exist, studies on the load transfer from the beams connected to these columns are scarce. Two experiments were carried out, expanding the datasets used for the development of the presented numerical model and demonstrating the applicability of this new solution.

From the calibrated numerical model, sensitivity tests were performed to reduce the processing time, which resulted in a representative and conservative numerical model. The numerical results were validated from the comparison with the relative force/displacement curves obtained experimentally, evaluating the initial stiffness, the maximum force value obtained in the analyzes and the deformed configuration of the models. The final model uses only 1/4 of the real models, due to its double symmetry, and can be used for study and design of the shear load transfer in CFST columns with slender composite section using shear connectors, which is a fundamental contribution to the development of new research and further development of a analytical model.

Rev. IBRACON Estrut. Mater., vol. 16, no. 1, e16108, 2023

14/16

ACKNOWLEDGEMENTS

REFERENCES

[1] Associação Brasileira de Normas Técnicas, *Projeto de Estruturas de Aço e de Estruturas Mistas de Aço e Concreto de Edifícios*, NBR 8800, 2008.

[2] Associação Brasileira de Normas Técnicas, *Projeto de Estruturas de Aço e de Estruturas Mistas de Aço e Concreto de Edificações com Perfis Tubulares*, NBR 16239, 2013.

[3] S. De Nardin and A. L. H. C. El Debs, "Shear transfer mechanism in connections involving concrete filled steel columns under shear forces," *Steel Compos. Struct.*, vol. 28, pp. 449–460, 2018.

[4] L. R. Santos, R. B. Caldas, L. F. Grilo, H. Carvalho, and R. H. Fakury, "Design procedure to bearing concrete failure in concrete-filled steel tube columns with bolted shear connectors," *Eng. Struct.*, vol. 232, pp. 1–12, 2021.

[5] U. Starossek, N. Falah, and T. Löhning, "Numerical analyses of the in concrete-filled steel tube columns," in *4th Int. Conf. Adv. Struct. Eng. Mechanics (ASEM'08)*, Jeju, Korea, 2008, pp. 2651–2666, http://dx.doi.org/10.12989/sem.2010.35.2.241.

[6] W. L. A. Oliveira, "Análise teórico-experimental de pilares mistos preenchidos de seção circula," Ph.D. dissertation, Esc. Eng. Estrut., USP, São Carlos, 2008.

[7] Y. Lu, Z. Liu, S. Li, and X. Zhao, "Effect of the outer diameter on the behavior of square rc columns strengthened with self-compacting concrete filled circular steel tube," *Int. J. Steel Struct.*, vol. 19, no. 3, pp. 1042–1054, 2019, http://dx.doi.org/10.1007/s13296-018-0185-9.

[8] American Institute of Steel Construction, *Specification for Structural Steel Buildings*, ANSI/AISC 360-16, 2016.

[9] H. S. Cardoso, "Estudo teórico-experimental de parafusos utilizados como dispositivos de transferência de carga em pilares mistos tubulares preenchidos com concreto," M.S. thesis, Esc. Eng., Dept. Eng. Estrut., Univ. Federal de Minas Gerais, Belo Horizonte, 2014.

[10] L. R. Santos, "Análise numérica de conectores parafusos em pilares mistos circulares preenchidos com concreto," M.S. thesis, Esc. Eng. , Dept. Eng. Estrut., Univ. Federal de Minas Gerais, Belo Horizonte, 2017.

[11] J. A. Prates, "Estudo de conectores de cisalhamento formados por parafuso com cabeça sextavada e rebite tubular com rosca interna para pilares mistos em perfis de aço formados a frio e concreto," M.S. thesis, Esc. Eng., Dept. Eng. Estrut., Univ. Federal de Minas Gerais, Belo Horizonte, 2017.

[12] J. G. Ribeiro No. and A. M. Sarmanho, "Experimental analysis of a mechanical shear connector in concrete filled steel tube column," *Ibracon Struct. Mater. J.*, vol. 10, no. 3, pp. 592–625, 2017.

[13] E. M. Xavier, J. G. Ribeiro No., A. M. C. Sarmanho, L. Roquete, and L. G. C. Paula, "Experimental analysis of bolts employed as shear connectors in circular concrete-filled tube colums," *IBRACON Struct. Mater. J.*, vol. 12, no. 2, pp. 337–370, Apr 2019.

[14] M. Y. Younes, H. M. Ramadan, and S. A. Mourad, "Stiffening of short small-size circular composite steel-concrete columns with shear connectors," *J. Adv. Res.*, vol. 7, no. 3, pp. 525–538, 2016, http://dx.doi.org/10.1016/j.jare.2015.08.001.

[15] Z. Tao, W. Li, B. L. Shi, and L. H. Han, "Behaviour of bolted end-plate connections to concrete-filled steel 2 columns," *J. Construct. Steel Res.*, vol. 134, pp. 194–208, 2017, http://dx.doi.org/10.1016/j.jcsr.2017.04.002.

[16] G. S. Veríssimo, "Desenvolvimento de um conector de cisalhamento em chapa dentada para estruturas mistas de aço e concreto e estudo do seu comportamento," Ph.D. dissertation, Dept. Eng. Estrut., Univ. Federal de Minas Gerais, Belo Horizonte, 2007.

[17] R. B. Caldas, R. H. Fakury, G. S. Veríssimo, F. C. Rodrigues, J. L. R. Paes, and A. L. R. Castro e Silva, *Análise Teórico-Experimental de Dispositivos de Transferência de Cargas em Pilares Mistos Formados por Tubos de Aço Preenchidos com Concreto, Projeto de Pesquisa*. Belo Horizonte, 2010.

[18] H. S. Cardoso, "Avaliação do comportamento de conectores constituídos por chapas de aço com recortes regulares — ênfase em conectores de geometria crestbond aplicados em pilares," Ph.D. dissertation, Esc. Eng., Dept. Eng. Estrut., Univ. Federal de Minas Gerais, Belo Horizonte, 2018.

[19] M. Pavlović, Z. Marković, M. Veljković, and D. Buđevac, "Bolted shear connectors vs. headed studs behaviour in push-out tests," *J. Construct. Steel Res.*, vol. 88, pp. 134–149, 2013, http://dx.doi.org/10.1016/j.jcsr.2013.05.003.

[20] European Standard, EN 1994-1-1:2004, 2004.

[21] L. R. Santos, "Conectores Crestbond aplicados a pilares mistos de seção esbelta," Ph.D. dissertation, Dept. Eng. Estrut., Univ. Federal de Minas Gerais, Belo Horizont, 2018.

Rev. IBRACON Estrut. Mater., vol. 16, no. 1, e16108, 2023

15/16

[22] O. P. Aguiar, "Estudo do comportamento de conectores Crestbond em pilares mistos tubulares preenchidos com concreto," Ph.D. dissertation, Esc. Eng., Dept. Eng. Estrut., Univ. Federal de Minas Gerais, Belo Horizonte, 2015.

[23] F. Tahmasebinia, G. Ranzi, and A. Zona, "Probabilistic three-dimensional finite element study on composite beam with steel trapezoidal decking," *J. Construct. Steel Res.*, vol. 80, pp. 394–411, 2013, http://dx.doi.org/10.1016/j.jcsr.2012.10.003.

Rev. IBRACON Estrut. Mater., vol. 16, no. 1, e16108, 2023

16/16